J|A|C|S
COMMUNICATIONS
Published on Web 05/31/2002

Connectivity of Features in Microlens Array Reduction Photolithography: Generation of Various Patterns with a Single Photomask

Hongkai Wu, Teri W. Odom, and George M. Whitesides*
Department of Chemistry and Chemical Biology, Harvard University, 12 Oxford Street, Cambridge, Massachusetts 02138

Received April 17, 2002

Periodic patterns with μm-scale features are important in applications ranging from media for data storage to substrates for high-density bioassay arrays. Typically, these patterns are written on surfaces using electron beams[1] or lasers,[2] and transferred into substrates using photolithography[1] or soft lithography.[3] The first two techniques use expensive apparatus; the second two require masks or masters, which are usually prepared by e-beam or laser writing. We have developed microlens array photolithography (MAP) as a technique that can be used to fabricate simple, repetitive features with minimal equipment and inexpensive masks. The features generated in MAP can be as small as 500 nm, and patterned over areas of cm^2.[4,5] MAP is a technique in which an array of microlenses positioned at a distance equal to their focal length from a layer of photoresist projects a cm-scale bright pattern into an array of microimages in photoresist. Unlike conventional projection lithographic techniques that form a single image of the chrome mask for each exposure and require precision optical systems and steppers to generate patterns over large areas,[6] MAP generates an array of images in a single exposure because each lens forms an image of the photomask. Although characteristics of the patterns formed by MAP are related to the symmetry of the microlens array, the images from these lenses can connect and overlap in different manners to generate a variety of patterns that are more complex than the microlens array.

Here we report that MAP, using a single mask and a single array of microlenses, can be used to generate multiple different patterns in photoresist; these patterns can have symmetries and periodicities different from that of the array of lenses. Forming a range of patterns using a single mask requires managing (i) the connectivity of the images produced by individual microlenses and (ii) the orientation of the photomask relative to the array of lenses during exposure.

The details of the fabrication of the microlens arrays and the optical setup have been described elsewhere[5] and are included in the Supporting Information. Briefly, the microlens array was fabricated by reflowing melted photoresist:[7] photographically patterned posts of photoresist were heated and melted to form lenses with the shape of a section of a sphere. An overhead projector was used as a broadband illumination source, and transparencies with cm-sized figures were used as photomasks (Figure 1A). Each microlens focused and formed an image of the figure of the mask into a photoresist-coated substrate. For a given value of the lattice spacing (a) of the lens array, when the overall size (l) of the figure on the mask was larger than a critical length l_c, the reduced images overlapped with each other to form a connected, continuous pattern (Figure 1B). The orientation of the mask relative to that of the microlens array is defined as the angle (α) between the direction along a lens to its nearest neighbors and that along a single arm of the cross (Figure 1C).

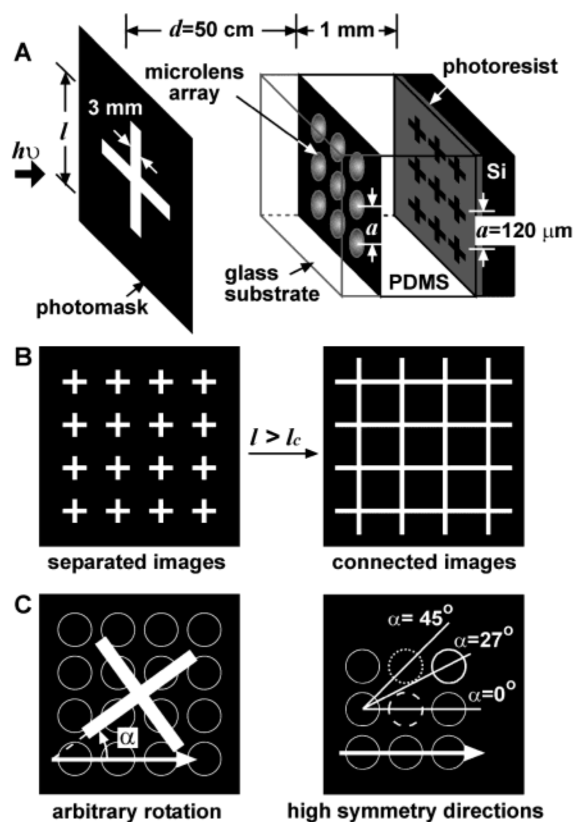

Figure 1. (A) Schematic diagram of microlens array photolithography (MAP). The thickness of the PDMS is exaggerated in the diagram to show the microlens array. In this experiment, the photomasks contain a single cross with line width of 3 mm and largest dimension l. (B) Scheme depicting how images overlap with each other when l becomes greater than a critical dimension l_c. (C) (left panel) Illustration showing the rotation of the cross on the mask at an arbitrary angle α, which is measured counterclockwise from the fixed orientation of the lens array (solid arrow). (right panel) Illustration showing the rotation angles along high-symmetry directions of the lens array. The images that overlap from neighboring lenses occur at $\alpha = 0°$ (dashed circle), 27° (bolded circle), and 45° (small-dashed circle).

To demonstrate the reduction capabilities of these lenses (100 μm in diameter, with $a \approx 120$ μm) (Figure 2A), we imaged a cross-shaped figure ($l = 8$ cm, $\alpha = 0°$) on the photomask into an array of microcrosses (100 μm across) in photoresist (Figure 2B). The overall size reduction was $\sim 0.8 \times 10^3$. The roughness at the edges of the microlenses (Figure 2A, inset, generated from a transparency mask[8]) did not degrade the reduction capability of the microlenses or the quality of the reduced images. The images of the crosses in photoresist were well separated (Figure 2B), and the pattern

* To whom correspondence should be addressed. E-mail: gwhitesides@gmwgroup.harvard.edu.

10.1021/ja020551k CCC: $22.00 © 2002 American Chemical Society

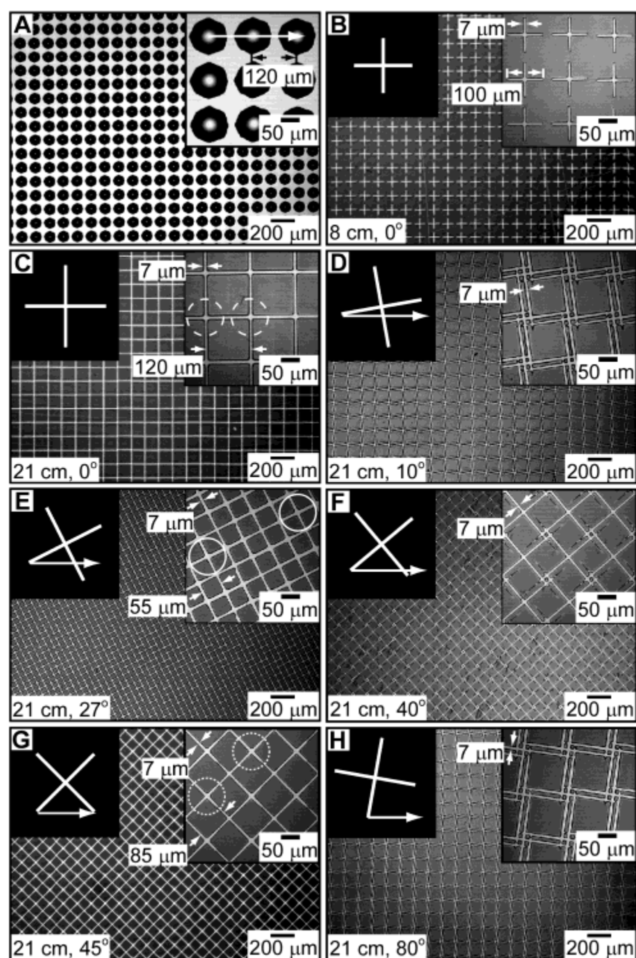

Figure 2. (A) Array of microlenses used to generate the patterns in (B)−(H). (B−H) Optical images of patterned photoresist using the lens array in (A). The numbers in the bottom left corners denote the overall size (l) of the cross on the mask (shown as the top left inset) and the orientation angle (α) of the mask relative to the microlens array (white lines with arrows indicate the direction along a lens to its nearest neighbor). The cross on all masks has a line width of 3 mm. The highlighted circles in (C), (E), and (G) indicate which lenses overlap to produce perfectly connected figures.

exhibited the same symmetry (D_{4h}) as that of the lens array. Areas as large as 2×2 cm^2 were patterned in photoresist without distortions.[5]

The size of an image formed by a lens increases in proportion to the size of the figure on the mask.[5] The critical length l_c of a mask to connect images along a high-symmetry direction of the lens array is the product of (i) the spacing of the lenses along that direction and (ii) the overall size reduction. For the microlens array in Figure 2A ($d = 50$ cm), l_c is ~10 cm and is given by the distance between lenses that are nearest neighbors ($a = 120$ μm) and the overall size reduction (0.8×10^3). This connectivity is evident in Figure 2C, where we used a photomask having a cross ($l = 21$ cm) with $l > l_c$. By orienting the cross along the direction of a translational repeat axis of the lens array ($\alpha = 0°$), we generated a grid of ~100 μm squares in photoresist with the same periodicity (120 μm) and symmetry (D_{4h}) as those of the lens array.

The ability to generate micropatterns having a *different* symmetry from, and a pitch increased over, that of the microlens array extends the capabilities of MAP. We demonstrate these capabilities in Figure 2D-H by changing the orientation of the masks ($l = 21$ cm) with respect to the lens array. The D_{4h} symmetry of the lens array guarantees that values of α between 0° and 90° generate all possible patterns.

Small rotations of the mask ($\alpha = 10°$, counterclockwise) generated a complex pattern in photoresist (Figure 2D). Although this pattern retained the C_4-rotational axis present in the microlens array, it eliminated the vertical planes of symmetry (σ_v) that existed in the lens array. When the figure on the mask was rotated to a high-symmetry axis of the array of microlenses ($\alpha = 27°$, Figure 2E), the image of the cross generated by one lens overlapped with that generated by a lens several lattice steps away (Figure 1C). This overlap formed a square grid having the same symmetry (D_{4h}) as the array of microlenses, but having a smaller unit cell (periodic spacing of 55 μm = (120 μm)[sin(27°)]). Further rotation of the mask ($\alpha = 40°$) generated a different, two-dimensional (2D) chiral pattern (Figure 2F) whose overall symmetry was again reduced to C_4. By rotating the mask so that images from next nearest neighbors were aligned ($\alpha = 45°$), we generated a square grid with D_{4h} symmetry but with a unit cell having another periodicity (85 μm = (120 μm)[sin(45°)]) (Figure 2E). For this experimental setup, the highest periodicity we can achieve is when $\alpha = 27°$. The next high-symmetry direction ($\alpha = 18.4°$) has a critical length of 30 cm; this value is larger than the size of the overhead projector and the size of the photomasks that we can print on standard transparency films.

Patterns that are generated by rotating the mask through an angle ($90° - \alpha$) are mirror images of those formed at the angle α. The mask oriented at $\alpha = 80°$ (Figure 2G) generated the mirror image of that shown in Figure 2D ($\alpha = 10°$).

This work demonstrates that a single array of microlenses can produce a variety of structures from a single mask by simply changing the relative orientation between the mask and the microlens array. Using a single mask and a single microlens array, we generated patterns that (i) are separated from each other, (ii) overlap with each other, (iii) are 2D chiral, and thus different from *both* the lens array and the mask, (iv) have a symmetry reduced from that of the lens array, or (v) have a smaller unit cell and smaller pitch than that of the starting lens array. This capability of MAP can be extended to many more combinations of patterns—both on the mask and in the microlens array. We believe that this technique provides a practical and flexible route to regular microstructures for physical and biological scientists who do not have routine access to conventional, high-resolution, photolithographic systems.

Acknowledgment. This work was supported by DARPA. T.W.O. thanks the NIH for a postdoctoral fellowship.

Supporting Information Available: Experimental details including fabrication of microlens arrays, microlens lithography, and pattern transfer (PDF). This material is available free of charge via the Internet at http://pubs.acs.org.

References

(1) Matsui, S. In *Handbook of Nanostructured Materials and Nanotechnologies*; Nalwa, H. S., Ed.; Academic Press: San Diego, CA, 2000; Vol. 3, pp 555−583.
(2) Metev, S. M.; Veiko, V. P. *Laser Assisted Micro-technology*; Springer: New York, 1998.
(3) Deng, T.; Arias, F.; Ismagilov, R. F.; Kenis, P. J. A.; Whitesides, G. M. *Anal. Chem.* **1999**, *72*, 645−651; Deng, T.; Wu, H.; Brittain, S. T.; Whitesides, G. M. *Anal. Chem.* **2000**, *72*, 3176−3180; Deng, T.; Tien, J.; Xu, B.; Whitesides, G. M. *Langmuir* **1999**, *15*, 6575−6581; Xia, Y.; Whitesides, G. M. *Angew. Chem., Int. Ed.* **1998**, *37*, 550−575.
(4) Wu, M. H.; Whitesides, G. M. *Appl. Phys. Lett.* **2001**, *78*, 2273−2275; Wu, M. H.; Paul, K. E.; Whitesides, G. M. *Appl. Opt.* **2002**, *41*, 2575−2585.
(5) Wu, H.; Odom, T. W.; Whitesides, G. M. *Anal. Chem.*, in press.
(6) Nonogaki, S.; Ueno, T.; Ito, T. *Microlithography Fundamentals in Semiconductor Devices and Fabrication Technology*; Marcel Dekker: New York, 1998; Rothschild, M.; Ehrlich, D. J. *J. Vac. Sci. Technol., B* **1988**, *6*, 1−17.
(7) Hutley, M.; Stevens, R.; Daly, D. *Phys. World* **1991**, *4*, 27−32.
(8) Qin, D.; Xia, Y. *Adv. Mater.* **1996**, *8*, 917−919.

JA020551K